REPORT #5: SCENARIOS FOR THE OPENING SCHOOLS DURING THE CHILEAN COVID-19 OUTBREAK

Authors: Claudia Álvarez, Alonso Cancino, Carla Castillo, Taco de Wolff, Pedro Gajardo, Rodrigo Lecaros, Jaime Ortega, Axel Osses, Héctor Ramírez, Nicolás Valenzuela.

Institutions: Centro de Modelamiento Matemático - CMM (Universidad de Chile), Group of Analysis & Mathematical Modeling Valparaiso - AM2V (Universidad Técnica Federico Santa María), Centro de Epidemiología y Políticas de Salud - CEPS (Universidad del Desarrollo).

Correspondence: carlacastillo@udd.cl, pedro.gajardo@usm.cl, axel.osses@dim.uchile.cl, hramirez@dim.uchile.cl

Date: May 7, 2020

ABSTRACT. In this document we model different scenarios related to the opening of schools in three regions of Chile: Metropolitan, Antofagasta and Valparaiso. For this purpose, we use the compartmental model introduced in our previous reports including now an age class structure. The contact matrices (contact indexes between age classes) used in our model are taken from [15], and the variation of activity due to the adopted measures in each region studied, are deduced from the Google activity report [2]. We simulate the progressive opening of schools (from May 11 until June 5) until reaching to 25%, 50%, 75%, and 100% of the school activity (with their implications in the other types of activities). These simulations are compared with the current situation in Chile (baseline), which we assume it corresponds to 0% of school activity. These scenarios are linked to future efforts in contact tracing and isolation of contacts (denominated cti strategy in previous reports), ranged from the *statu quo* scenario (current situation) to very strong efforts in cti. As outputs of our model we present the hospitalization demands (non critical and critical beds) in each considered scenario.

CONTENTS

1. Introduction

Since the emergence and spread of COVID-19 outbreak throughout the world, countries have implemented different containment and mitigation policies in order to flatten the peak of critical cases and, consequently, trying to prevent, as far as possible, the collapse of their health systems [12]. Public health policy responses to the pandemic aim both to limit the number and duration of social contact, and include measures such as early detection of cases and tracing and isolating infected individual's contacts, full or partial lockdowns, and school closures among others [12].

After the confirmation of the first cases in early March [9], school closures was one of the first measures implemented in Chile as a response to the COVID-19 outbreak. Indeed, face-to-face pre-schools and school classes were suspended, originally for two weeks, in March 16, and the suspension has been extended, including the advancement of winter break, to date. However, in the recent days, much has been discussed regarding the need of a "safe return" or of returning to a "new normality", which implies, for instance, gradually re-opening schools and commerce, and ending of lock-downs. Thus, while contact tracing and isolation as well as lockdown strategies have been analyzed in our previous reports [6, 7, 5], this report analyses the re-opening of schools, one of the measures considered by the authorities. *Comité Asesor COVID-19 Chile*, the advisor committee to the Chilean government, in its memorandum of April 6 advocated for territorial gradualness in the opening of schools in different regions or municipalities specific, and proposed to consider specific indicators for this matter, such as reporting an effective reproductive number lower than 1.5 at the national level; absence of new cases for at least 14 days (a complete incubation period) or sustained reduction in the number of new cases in the last 14 days; and, less than 10% of the cases not possible to trace [3]. Furthermore, *Comité Asesor COVID-19 Chile* recommended gradualness in the opening of each school, strengthening social distance measures, respiratory hygiene and school disinfection [3].

The purpose of this report is to estimate the maximal ICU and normal beds demand in the context of COVID-19 outbreak, presenting different scenarios of school re-opening in three Chilean regions: Metropolitan (Santiago), Antofagasta and Valparaiso, which have

an increasing number of new cases per day and their corresponding effective reproductive numbers are greater than one. We use an extension of the compartmental epidemiological model introduced in Report #2 [6] that considers an age structure and, therefore, allows the representation of school interactions.

2. Description of the model

The disease spread within a particular city or region has been modeled using a deterministic compartmental model (see, for instance [4] and references therein). In our previous reports [8, 6, 7, 5], our team has implemented this approach to the COVID-19 outbreak in Chile. The deterministic and compartmental approach that we develop has some important advantages with respect to other approaches: among them, the most important are the simplicity and the rapidity to obtain results that can provide key insights and data for being used later in more complex models (e.g., stochastic, with interconnection between cities/districts, etc.).

The main difference with the model used in our previous reports has been to incorporate here an age class structure. Thus, the population is distributed into nine age classes and the population in each age class is distributed into eight groups corresponding to different stages of the disease, as considered in [6, 7, 5]:

- **Susceptible** (denoted by S): Persons not infected by the disease, but able to be infected by the virus.

- **Exposed** (denoted by E): Persons in the incubation period after being infected by the disease. In this stage, persons **do not have symptoms but they can infect other people** [13] with a lower probability than people in the infectious compartments described below.

- **Mild infected or subclinical** (denoted by I^m): Persons infected that can infect other people. Persons in this stage are asymptomatic or present mild symptoms, **they are not detected and then not reported by authorities**[1]. At the end of this stage, they pass directly to recovered state.

- **Infected** (denoted by I): Persons infected that can infect other people. Persons in this stage develop symptoms and **are detected and then reported by authorities**.People in this stage can recover or pass to some hospitalized state.

- **Recovered** (denoted by R): People that survive the disease, **is no longer infectious and have developed immunity to the disease**.

- **Hospitalized** (denoted by H): Persons hospitalized in basic facilities. People in this stage can infect other people. **After this stage, people recover, pass to use a ICU bed,**

---

[1] This was the situation until April 28, when Chilean government has modified the way to compute and report the daily number of infected [9]. They now report symptomatic and asymptomatic cases due to a change in the detection strategy.

or die[2]. We assume that persons in this stage are strongly isolated and, consequently, they cannot infect other people.

- **Hospitalized in ICU beds** (denoted by H^c): People hospitalized in ICU beds. People in this stage can infect other people. After this stage, **people die or are hospitalized in basic facilities**. We assume that persons in this stage are strongly isolated and, consequently, they cannot infect other people.

- **Dead** (denoted by D): People who did not survive the disease.

The choice of the above stages and the transition between them are because our main purpose is to estimate the **maximal demand of critical (ICU) and not critical beds**. For this reason we are modeling that all people that need a hospitalization will pass by stage H or H^c without any constraint of availability.

For the age class structure we consider nine clases: [0-9], [10-19], [20-29], [30-39], [40-49], [50-59], [60-69], [70-79], [80+]. Thus, for each class $i \in \{1, 2, \ldots, 9\}$, the vector of state variables $\mathbf{x}_i = (S_i, E_i, I_i^m, I_i, R_i, H_i, H_i^c, D_i)$ has eight components corresponding to the stages of the disease described above.

The evolution of state variables in the age class $i \in \{1, 2, \ldots, 9\}$ is described by the following system of ordinary differential equations:

$$
(1) \quad
\begin{cases}
\dot{S}_i & = \mu_b N_i - S_i \overbrace{\left(\sum_j \dfrac{\alpha(t) p_E C_{ij} E_j + \alpha(t) p_{I^m} C_{ij} I_j^m + \delta\, p_I C_{ij} I_j}{N_j} \right)}^{\Lambda_i(\mathbf{x}, C): \text{ rate of contagious}} - \mu_d S_i \\[4mm]
\dot{E}_i & = S_i \Lambda_i(\mathbf{x}, C) - (\gamma_E + \mu_d) E_i \\[2mm]
\dot{I^m}_i & = (1 - \phi_{EI}) \gamma_E E_i - (\gamma_{I^m} + \mu_d) I_i^m \\[2mm]
\dot{I}_i & = \phi_{EI} \gamma_E E_i - (\gamma_I + \mu_d) I_i \\[2mm]
\dot{R}_i & = \gamma_{I^m} I_i^m + \phi_{IR} \gamma_I I_i + \phi_{HR} \gamma_H H_i - \mu_d R_i \\[2mm]
\dot{H}_i & = (1 - \phi_{IR}) \gamma_I I_i + (1 - \phi_{H^c D}) \gamma_{H^c} H_i^c - (\gamma_H + \mu_d) H_i \\[2mm]
\dot{H^c}_i & = (1 - \phi_{HR} - \phi_{HD}) \gamma_H H_i - (\gamma_{H^c} + \mu_d) H_i^c \\[2mm]
\dot{D}_i & = \phi_{HD} \gamma_H H_i + \phi_{H^c D} \gamma_{H^c} H_i^c.
\end{cases}
$$

The structure of the model is depicted in Figure 1.

The parameters are the same as in the previous reports (see [6, 7, 5]) but could be dependent on the age class $i \in \{1, 2, \ldots, 9\}$; see Section 2.2. This is considered in the simulations but not represented in the above system in order to simplify the presentation of this new model. In previous reports we used the parameter ϕ_D corresponding to the fraction of people in H^c (ICU bed) that die. Now this parameter is replaced by ϕ_{HD} and

---

[2]The possibility to die at this stage, not considered in our previous reports, is included here because an important number of deaths in Chile occurred when patients are hospitalized in normal beds.
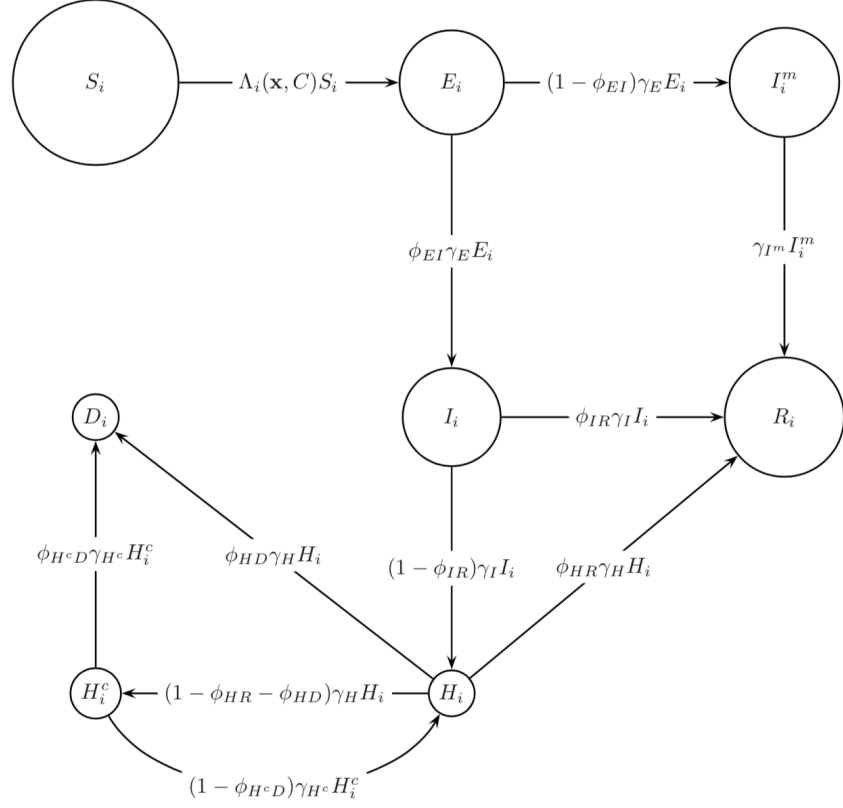
FIGURE 1. **Structure of the mathematical model for the dynamics of COVID-19 in an isolated region for the age class i.** Each circle represents a compartment. Susceptible individuals (S), and different disease states: exposed (E), mild infected (I^m), infected (I), recovered (R), hospitalized (H), hospitalized in ICU beds (H^c), and dead (D). Natural natality and mortality flows are not represented.

ϕ_{H^cD} because here we are considering the possibility to die at the hospitalized stage H. This situation has been observed for the oldest population in Chile and abroad; see, for instance, [11].

Entries C_{ij} in the matrix $C = (C_{ij})_{i,j \in \{1,\dots,9\}}$ represent the contact rates between age groups, and they are proportional to daily contacts that an infected individual in age class j has with susceptible individuals of age class i, as described in the next section. The function $0 \leq \alpha(t) \leq 1$ stands for the control mitigation strategy of *contact tracing and isolation of contacts*, called *cti* in [5, 7], affecting the infection rate of exposed and mild infected individuals. Therefore, with different choices of function $\alpha(t)$ we model different efforts related to cti strategy.

2.1. **Contact matrices.** We assume that the contact matrix $C = (C_{ij})_{i,j \in \{1,\dots,9\}}$ for exposed individuals (people in stage E) is equal to the one for infected subclinical individuals (people in I^m) and that the contact matrix for infected symptomatic (people in I) is also the same with a reduction factor $\delta = 0.2$ (because, as in previous reports [7, 5], we assume that infected people are more isolated). This allows considering a single contact matrix

C from which all others are computed. This contact matrix is divided into four-contact *environments*: work contacts, school contacts, home contacts and other contacts:

$$(2) \qquad C = C_{\text{work}} + C_{\text{home}} + C_{\text{school}} + C_{\text{other}}.$$

This matrix decomposition is taken from [15] where estimations for different countries, including Chile, are provided for sixteen age classes. Here we interpolated to nine age classes: [0-9],[10-19],[20-29],[30-39],[40-49],[50-59],[60-69],[70-79],[80+] (see Figure 2).
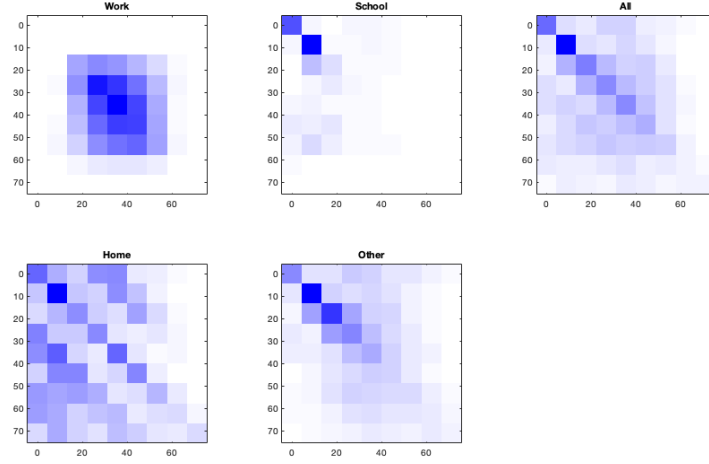

FIGURE 2. Contact matrices for the considered environments: work, school, home, other and their sum, considering nine age classes corresponding to Chile [15].

Our approach for adjusting the model and evaluate future scenarios consists in applying to each matrix in (2) some suitable time dependent factors (f_{work}, f_{home}, f_{school}, f_{other}). These factors are described and justified below.

Therefore, they all are introduced in order to obtain a time dependent contact matrix C given by:

$$(3) \qquad C = (1 + f_{\text{work}})C_{\text{work}} + (1 + f_{\text{home}})C_{\text{home}} + f_{\text{school}}C_{\text{school}} + (1 + f_{\text{other}})C_{\text{other}}.$$

These dynamic factors $f_{\text{environment}}$ are intended to simulate variations in contact activity with the corresponding effect in the infection rate. In order to establish reasonable values for these factors we use as proxy values the variations in activity of the population from the Google activity reports 2020 [2] for different regions in our country. We show in Table 1 factors $f_{\text{environment}}$ after the adopted measures in the Metropolitan Region.

We consider residential activity as a proxy for home contacts, workplaces activity as a proxy for work contacts and some combination of: retail and entertainment (48%), transit (24%), parks (8%) and pharmacy and groceries (20%) as a general proxy for the variation in strength for other contacts. **Our main assumption is that the variation in the rate of contacts is proportional to the variation in the corresponding associated**

activity. For the amplitude of this variations we consider as a reference the basal activity at the beginning of March 2020 when no mitigation actions had been applied in the country. In Figure 3 we show the evolution of home, work, school and other contact factors obtained from Google activity reports 2020 [2] for the Metropolitan Region.

Notice that, in practice, we may also include two diagonal matrices D_{home} and D_{other}, that appear in (3) multiplying matrices C_{home} and C_{other}, respectively, in order to enhance the colateral impact in younger people (0 to 20 years old for instance). However, these factors have been omitted here for the sake of simplicity.
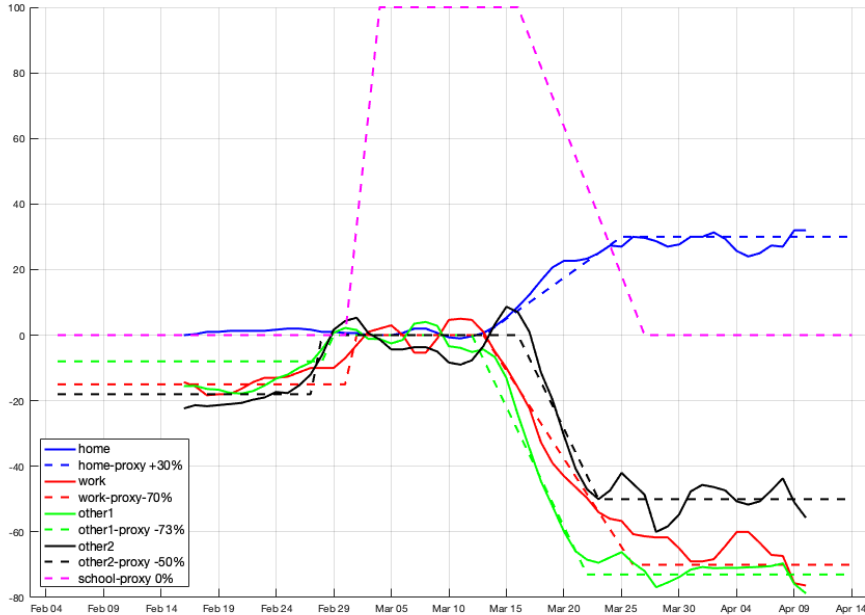

FIGURE 3. Evolution of home, work, school and other contact factors obtained from Google activity reports 2020 [2] (3 day average) taking as reference the activity of March 2020 for the Metropolitan Region. Here, "Home" stands for residential activity, "work" for workplaces activity, "other1" is a combination of retail and recreation (60%), transit stations (30%) and parks (10%) and "other2" corresponds to pharmacy and groceries activity. Our environment "Other" is a combination of "other1" (80%) and "other2" (20%), which in turns corresponds to percentages declared in Section 2.1.

For the time dependency of the activity related factors, sometimes we will consider step type changes, linear or sometimes quadratic behavior.

2.2. **Parameters.** For simplicity, we assume that most of the parameters in the model are no age dependent, except for the following that we consider critical for capturing the age dependency dynamics:

- population fraction $f_i = 1/N_i$ and mortality rate by age μ_d are taken from Census 2017 in Chile.

Factor	Activity proxy	Variation	Source
f_{home}	residential	From 0% to +30%	[2]
f_{work}	workplaces	From 0% to -70%	[2]
f_{other}	retail, entertainment, transit, parks pharmacy and groceries	From 0% to -68%	[2]
f_{school}	school	From 100% to 0%	modeling team

TABLE 1. Variation of activity and contact factors for the different environments due to the implementation of mitigation measures between March 1 and April 15 2020 in the Metropolitan Region [2].

- rates ϕ_{HD}, ϕ_{HR} and ϕ_{H^cD} and fraction of infected asymptomatic ϕ_{EI} by age are taken from [16].
- inverse of stage duration times γ_H, γ_{H^c} and fraction of infected that recover ϕ_{IR} by age are taken from [11].

The other parameters: inverse of stage duration times γ_E, γ_{I^m}, infection probabilities p_E, p_I, p_I^m and other parameters are considered the same for all age compartments and they are chosen following the recommendations and assumptions of our previous reports [5, 7] for the single-age model.

2.3. **Reproductive numbers.** Using the next generation matrix method (see [10]) and by neglecting the effect of birth and mortality rates, we can estimate the basic reproductive number by age:

$$\mathcal{R}_0^i = \alpha\rho(c)\left(\frac{p_E}{\gamma_E} + \frac{(1-\phi_{EI}^i)p_{I^m}}{\gamma_{I^m}} + \frac{\phi_{EI}^i p_I}{\gamma_I}\right)$$

where $\rho(c)$ is the leading eigenvalue (spectral radius) of the *normalized contact matrix* whose entries are given by $c_{ij} = C_{ij}N_i/N_j$. The effective reproductive number by age is then estimated by:

$$\mathcal{R}_e^i = \mathcal{R}_0^i S_i/N_i.$$

Then, the aggregate reproductive numbers are simply set as follows

$$\mathcal{R}_0 = \sum_i f_i \mathcal{R}_0^i, \qquad \mathcal{R}_e = \sum_i f_i \mathcal{R}_e^i,$$

where f_i are the population fractions introduced above.

3. CALIBRATION AND VALIDATION OF THE MODEL

We adequate the calibration process reported in [5, 7] to adjust the parameters and initial conditions of our model. For this, we consider available data since March 2 to April 27, 2020 [9]. The parameters of the model are thus fit to the following data: accumulated and daily number of infected reported, the effective reproductive number (by using the formulas stated in the previous section), and the accumulated and daily deaths. In addition, we need to take into account the impact of the different mitigation actions occurred during March in the different regions (namely, social distancing, curfew, closing schools and partial lockdowns). For this, we have taken as proxies the variation of activities in Google activity reports (see

data associated to Metropolitan region in Figure 3). The simulations are performed and plotted since March 10 for validation purposes. See Figure 4.
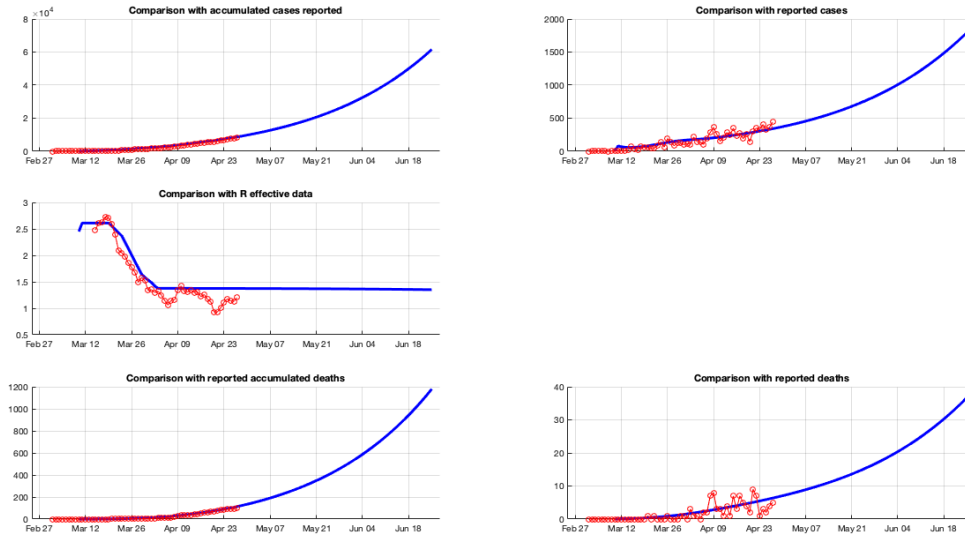

FIGURE 4. Calibration and validation of the age-structured model for Metropolitan Region using the following data: accumulated and daily number of infected reported, daily effective reproductive number, and accumulated and daily deaths.

Also, as said before, our model is calibrated to match (among other quantities) the reported cases of infected symptomatic, but this quantity is in practice under-reported. Indeed, based on the methodology introduced in Russell et al [17], we estimate that the reported fraction of infected symptomatic in the considered period in Chile is about 45%. This correction is considered in our calibration process. This under-reporting may also affect the estimations in magnitude of all the other variables in the system. In particular, this may lead to an underestimation of the number of hospitalizations H and H^c (and, therefore, deaths D). However, since this underestimation is highly nonlinear, and not fully understood yet, we have decided to report the values obtained by our model without considering any additional correction factor. This important issue will be taken into account in future analysis.

Of course, the longterm results for our baseline simulations are highly dependent of the current value of the effective reproduction number and of its future evolution, which in turn depends on the mitigation factor $\alpha(t)$ applied to the dynamic. We thus consider three cases: *current measures*, where no improvement is made since the current situation (i.e., $\alpha(t) = 1$), *moderate intensity*, where we assume that $\alpha(t)$ decreases from 1 to $4\delta = 0.8$ (being $\delta = 0.2$ the isolation factor between subclinical and symptomatic infected introduced in [5]), and *high intensity*, where we assume that $\alpha(t)$ decreases from 1 to $3\delta = 0.6$. As already said, these three cases are related to different levels of efforts in the implementation of cti

strategies. Hence, the first case can be interpreted as to maintain the current low-intensity cti strategy, the second one as to increase it to a moderate intensity, and the third one as to target the implementation of a cti strategy with a (very) high intensity. We simulate these three baseline cases for a 12 months period, starting at March 10. The results are reported in figures 5 and 6.
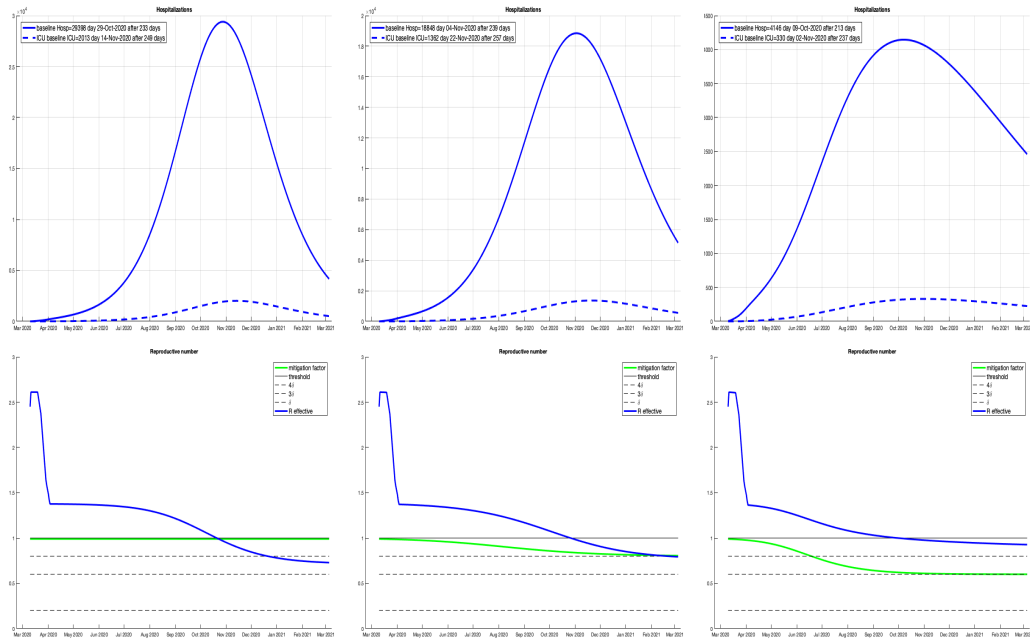

FIGURE 5. Simulation results for Metropolitan Region order from current measures to high intensity (from left to right); Evolution of hospitalizations are shown on top and of effective reproductive number on the bottom.

In Figure 5 we see that the cases when we maintain the currently adopted cti strategy and those when we increase to a moderate intensity one exhibit similar behavior of their demands for hospitals beds, only their amplitudes differ. When a high intensity cti strategy is applied, the numbers of required beds are much less in their respective peaks.
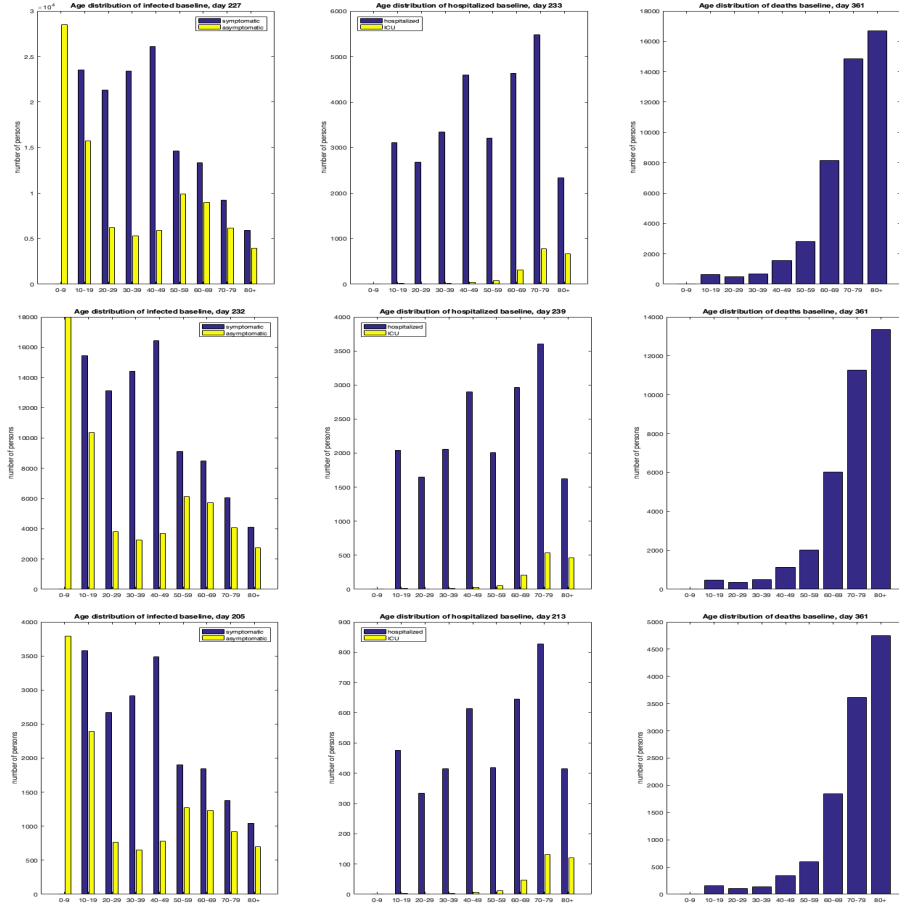
FIGURE 6. Simulation results for Metropolitan region for the three cases: current measures (top row), moderate intensity (middle row) and high intensity (bottom row); age distribution of infected symptomatic and asymptomatic is shown in the left column, of hospitalized in normal beds and ICU beds in the middle column, and of death in the right column.

In Figure 7 we can visually compare the distribution, by age, of the accumulated infection cases and of deaths reported for the whole country with the corresponding age distributions obtained with our model. We are not able to display these distributions for each region because that data is not available at a regional level. However, we can verify that the main tendencies are recovered in our simulations: more cases of symptomatic in mid age population and increasing death risk for older population.
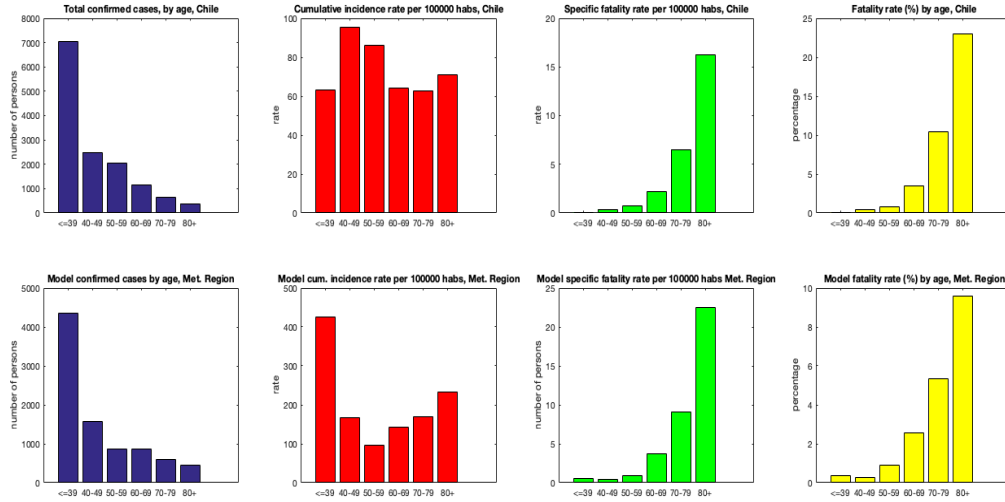
FIGURE 7. First row: age distribution of total confirmed cases, cumulative incidence rate, specific fatality rate and fatality rate at national level until April 27, 2020. Second row: comparison with the model for the same date for the Metropolitan Region.

4. SIMULATIONS OF A GRADUAL OPENING OF SCHOOLS

For the three level of cti strategy intensity (current measures, moderate and high intensity) described in the precedent section, we simulate a gradual opening of schools. This is carried out from May 11 2020 to June 5 2020 by varying the contact factors of schools, in a linear way, from 0% to a given final activity level parametrized by p. The latter takes the values 0.25, 0.5, 0.75 and 1 in our simulations, representing the percentages 25%, 50%, 75% or 100%, respectively, related to the final level of the school opening (i.e., percentages for the attendance of students). Those values are then maintained in the rest of the simulation (that is, from June 5 to the end of the simulation). Since opening schools decreases the level of contact at home (because students are no longer there) and increases other way of contacts (mainly because an increment of contacts due to the transport of students), we also consider linear variations of the respective factors. Then, when simulating a school opening scenarios (characterized by its final value p), we consider linear variations of f_{home}, from $+30\%$ to $+(1 - 2p/3)30\%$, and of f_{other}, from -60% to $-(1 - p/3)60\%$. The final value for the factor "home" gets a maximum value of -40%, when $p = 1$, which corresponds to assume that the initial increment of this factor was explained in a proportion $1/3$ by the presence of students at home (so, the rest may be explained by the adults working at home, among other possibilities), while the final value for the factor "other" gets a maximum value of -40%, when $p = 1$. This value in turn corresponds to a difference of 20% for this factor, which is the observed difference of the activity "other" in Figure 3 when the schools at the end of February 2020. All these scenarios, as well as our baseline, are summarized in Table 2 for Metropolitan region and are shown in Figure 8.

Comparison of numbers of required ICU beds at the peak for different scenarios

Scenario	f_{school}	f_{home}	f_{other}	f_{work}
Baseline (ICU beds)	0%	+30%	−60%	−70%
Scenario 1	0% to 25%	+30% to 22.5%	−60% to −55%	unchanged
Scenario 2	0% to 50%	+30% to 15%	−60% to −50%	unchanged
Scenario 3	0% to 75%	+30% to 7.5%	−60% to −45%	unchanged
Scenario 4	0% to 100%	+30% to 10%	−60% to −40%	unchanged

TABLE 2. Evolution of contact/environment factors for the Metropolitan Region when different schools opening scenarios are applied.
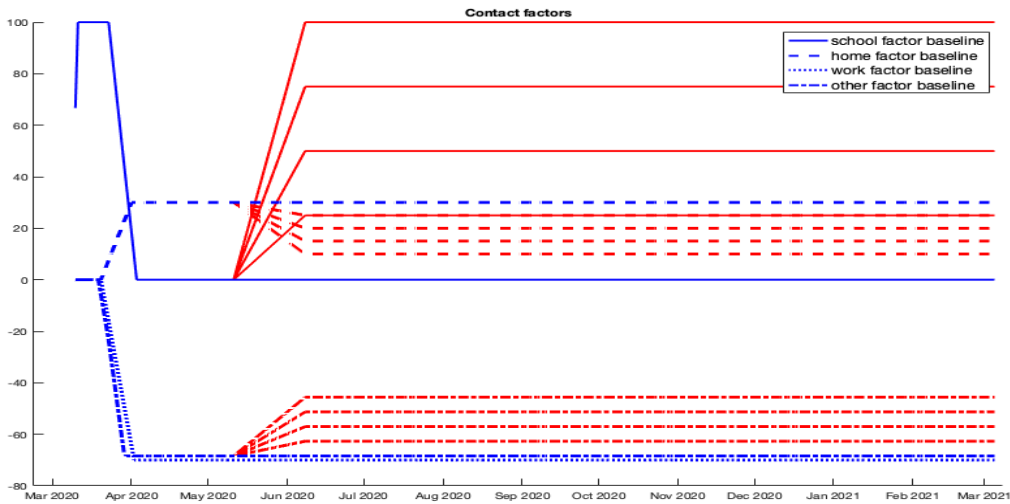

FIGURE 8. Evolution of contact/environment factors for each simulated scenario. Blue lines stand for our baseline situation and red lines for the variations due to the four different scenarios: 25%, 50%, 75% and 100% of gradual school opening.

Finally, the simulation period is 12 months, starting at March 10 2020. The results are shown in figures 9 and 10. The analysis above is reported only for Metropolitan region. For the other regions we just report the study of the peaks of ICU beds for the different scenarios; see tables 3, 4, and 5.
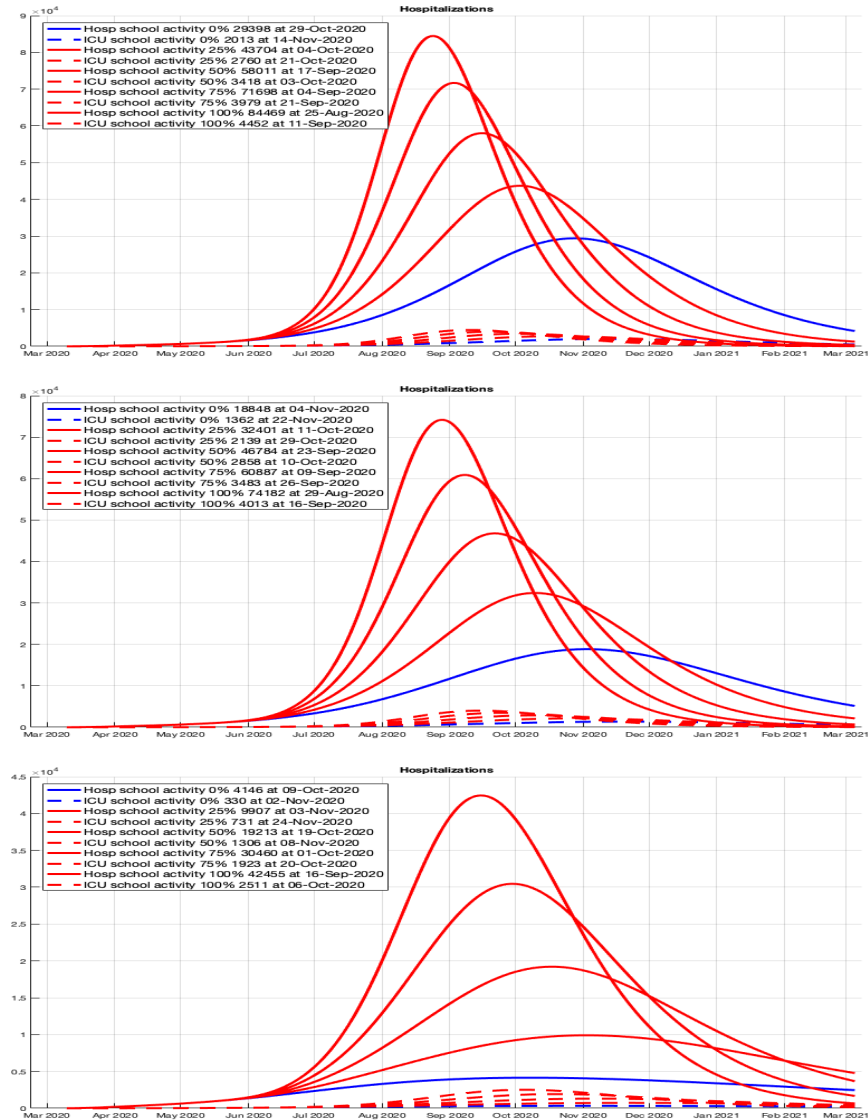
FIGURE 9. From top to bottom: current measures, moderate intensity and high intensity cti efforts; The evolution of the hospitalization demands (normal and ICU beds) in Metropolitan Region is plotted in red for each of the four opening schools scenarios (25%, 50%, 75% or 100%) and in blue for our baseline (0%); The higher the percentage, the higher (and earlier) the maximum.

As a general result, we can observe that, as expected, when a higher final value p is targeted (that is, when a more ambitious scenario is considered), higher is the size of the peak in both, normal and ICU beds. On the other hand, regarding the date of those peaks, they occur earlier as long as we target a higher value of p for the threes cases (current cti measures, moderate and hight intensity). We observe the same qualitative behavior in the simulations for Antofagasta and Valparaiso regions but, for the sake of space, their graphics are omitted.
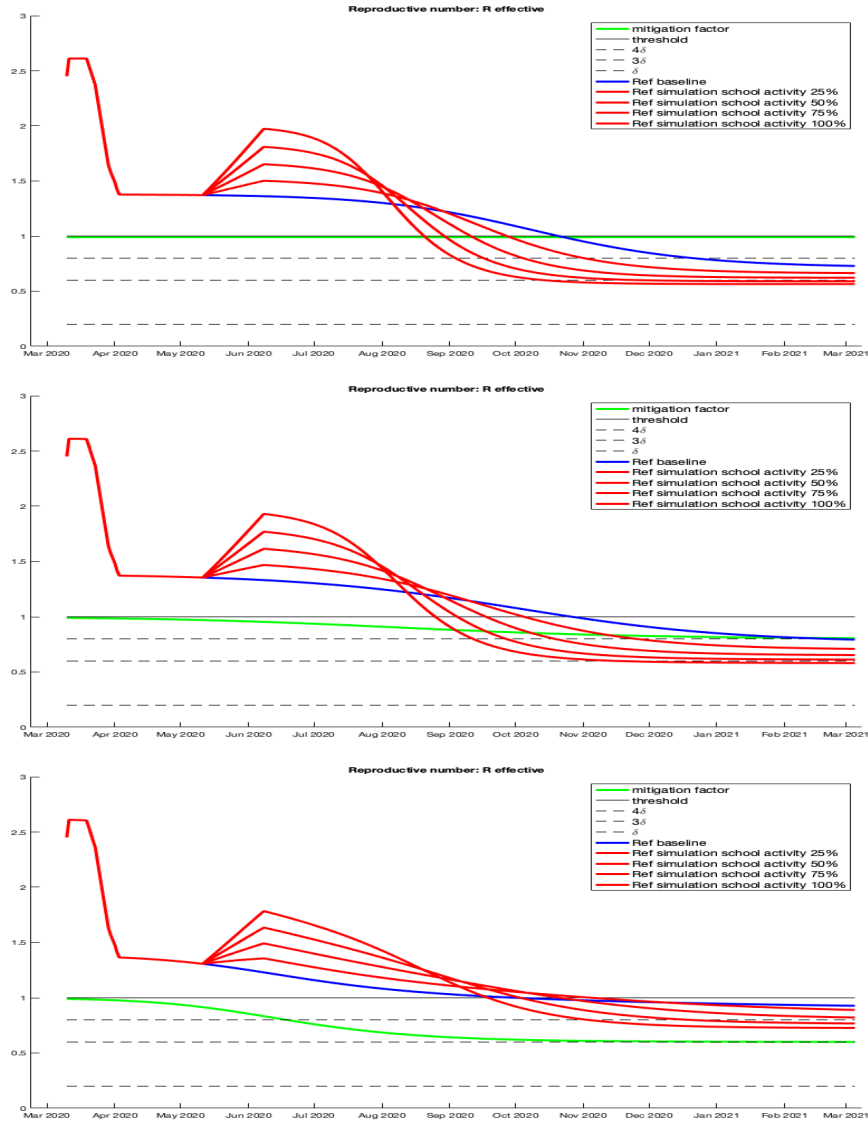
FIGURE 10. From top to bottom: current measures, moderate intensity and high intensity cti efforts; The evolution of effective reproductive numbers in Metropolitan Region is plotted in red for each of the four opening schools scenarios (25%, 50%, 75% or 100%) and in blue for our baseline (0%); The evolution of our mitigation factor $\alpha(t)$ is plotted in green.

In tables 3, 4, and 5 we show the increment, with respect to the baseline, of maximal required ICU beds for Metropolitan, Antofagasta and Valparaiso regions respectively, in each simulated scenario.

Incremental maximal ICU demand in Metropolitan Region

Scenario/cti intensity	Current measures	Moderate intensity	High intensity
Baseline	2013	1362	330
Scenario 1 (25%)	2760 (37%)	2139 (57%)	731 (122%)
Scenario 2 (50%)	3418 (70%)	2858 (110%)	1306 (296%)
Scenario 3 (75%)	3979 (98%)	3483 (156%)	1923 (483%)
Scenario 4 (100%)	4452 (121%)	4013 (195%)	2511 (661%)

TABLE 3. Percentage of increment of ICU beds, with respect to the baseline, for Metropolitan Region when different schools opening scenarios are applied and for different effort levels in the cti strategy.

Incremental maximal ICU demand in Antofagasta Region

Scenario/cti intensity	Current measures	Moderate intensity	High intensity
Baseline	267	164	42
Scenario 1 (25%)	372 (39%)	260(59%)	75 (79%)
Scenario 2 (50%)	483 (81%)	370 (126%)	132 (214%)
Scenario 3 (75%)	596 (123%)	486 (196%)	210 (400%)
Scenario 4 (100%)	708(165%)	603 (268%)	304 (624%)

TABLE 4. Percentage of increment of ICU beds, with respect to the baseline, for Antofagasta Region when different schools opening scenarios are applied and for different effort levels in the cti strategy.

Incremental maximal ICU demand in Valparaiso Region

Scenario/cti intensity	Current measures	Moderate intensity	High intensity
Baseline	70	23	21
Scenario 1 (25%)	216 (209%)	37 (61%)	22 (5%)
Scenario 2 (50%)	421 (501%)	115 (400%)	24 (14%)
Scenario 3 (75%)	663 (847%)	276 (1100%)	31 (48%)
Scenario 4 (100%)	925 (1221%)	500 (2074%)	59 (181%)

TABLE 5. Percentage of increment of ICU beds, with respect to the baseline, for Valparaiso Region when different schools opening scenarios are applied and for different effort levels in the cti strategy.

As expected, we observe the increment of required ICU beds when we target larger percentages of schools activity. In these tables, we can compare the percentage of the increment in the ICU demand with the percentage of opening schools in order to evaluate if in one scenario, these proportions are similar.

From Table 3 (Metropolitan Region) we note when a high intensity cti strategy is implemented, the value at the peak increases almost eight times when we target to fully open all the schools in just one month, and increase in almost six times when we target the 75% scenario. On the other hand, when lower cti efforts level are considered, the respective

increments are important even for the less demanding 25% scenario. So, in the case when a high intensity cti strategy may be difficult to implement, it seems reasonable to keep the schools closed or, at most, to target the less demanding 25% scenario during May.

For Antofagasta Region (see Table 4) the analysis is similar. Indeed, the increments (percentages) are similar to Metropolitan Region.

Finally, in Valparaiso Region (see Table 5) we observe a more extreme situation. In the case when a high intensity cti strategy is implemented, the value at the peak increases in a very smooth way. Under this strategy one could target even to fully open all the schools in just one month with a "moderate" increment of %181, which coincides with the current maximal ICU beds capacity in that region (about 60 ICU). However, when lower cti efforts level are considered, the respective increments are proportionally very high, even for the less demanding 25% scenario, and actually extremely high for more ambitious scenarios (e.g., 1221% and 2074% for scenario 4). Summarizing, this region exhibits a huge qualitative difference between high intense cti strategy and the others.

5. Recommendations and final remarks

Results obtained with compartmental models approach as the introduced in this document are very sensitive to some key parameters. Indeed, it is known (see [14]) that the parameter identification of an outbreak model before the peak can produce large errors in the outputs. Nevertheless this kind of approach is useful to observe the direction of changes associated with different strategies. In this report we have focused our attention in the impact of re-opening schools.

As said by the *Comité Asesor COVID-19 Chile*, the advisor committee to the Chilean government, in its memorandum of April 6, 2020 [3], the closure of schools is one of the most used non-pharmaceutical measures to reduce the spread of communicable diseases during epidemics. A systematic review on school closure during coronavirus outbreaks can be found in [18]. In [1] the CDC in US declares that available modeling data indicate that early, short to medium closures do not impact the epidemiological curve of COVID-19 or available health care measures (e.g., hospitalizations). There may be some impact of much longer closures (8 weeks, 20 weeks) further into community spread. Their models also show that other mitigation efforts have more impact on both spread of disease and health care measures. The experience abroad shows that those places who closed school (e.g., Hong Kong) have not necessarily had more success in reducing spread than those that did not (e.g., Singapore). The latter was actually also informed by the *Comité Asesor COVID-19 Chile* in the memorandum mentioned above. However, the same *Comité Asesor COVID-19 Chile* stress out the difficulty to compare the effect of closuring schools in different situations. Consequently, they consider specific indicators for territorial gradualness in the opening of schools, namely: reporting an effective reproductive number lower than 1.5 at the national level; absence of new cases for at least 14 days (a complete incubation period) or sustained reduction in the number of new cases in the last 14 days; and, less than 10% of the cases not possible to trace [3].

These conditions are not currently satisfied in the regions studied in this document and, therefore, following the *Comité Asesor COVID-19 Chile* advice, it would be not recommendable to lift the closure of schools. This is coincident with the results obtained with our model. However, our results open the possibility to partially lift it provided intense cti strategies are adopted. Here below we detail our recommendations.

Recommendations

The most important recommendation is to increment the efforts on cti strategies. As we analyzed in our previous reports the impact of cti strategy is the highest among the strategies modeled by our group. Thus, higher efforts in cti strategy would imply lower impact of schools re-opening. In specific for each region analyzed:

- **Metropolitan Region (Santiago):** Applying a high intensity cti strategy, authorities can asses some reasonable scenarios. For instance, it can be targeted to come back to 50% of the school activities in the following month with the risk of tripling the number of required ICU beds at its peak (if no other measures are implemented), or to consider a more risk-aversion behavior and target only to comeback to 25% of the school activity, for which this increment is "only" 122% more. When the implementation of such strategy is difficult, we should consider to maintain the current measures or, at most, to be able to implement a moderate intensity cti strategy. In such case, even the first scenario can imply more than two thousand required ICU beds. Consequently, in the case when it is not possible to apply a high intensity cti strategy we recommend to keep the schools closed in Metropolitan Region or, at most, to target the 25% scenario at the beginning of June.

- **Antofagasta Region:** In this region we observe a similar situation. Indeed, the increments (percentages) of maximal ICU beds demand are similar to Metropolitan Region. For this reason in case when a high intensity cti strategy is not being fully implemented, we recommend to keep the schools closed or, at most, to target the 25% scenario at the beginning of June.

- **Valparaiso Region:** This region exhibits an extreme difference, from the qualitative viewpoint, between high intense cti strategy and the others. In the case when a high intensity cti strategy is implemented, authorities could even target to fully open all the schools in just one month with a "moderate" increment of %181, which coincides with the current maximal ICU beds capacity in that region (about 60 ICU beds). However, when lower cti efforts level are considered, the respective increments are proportionally very high even, even for the less demanding 25% scenario. This region has not been in quarantine yet and has recently suffered an increment of the effective reproductive number, posterior to long weekends (possibly due to the visit of people from other regions with more infected cases, such as Metropolitan one). Consequently, it seem very unlikely to implement a high intense cti strategy in the short term. Moreover, in order to be effective, a cti strategy should be applied together by other isolation measures, such as to strongly restrict the access to this region from others. In consequence, and since the variations are very important when lower cti efforts level are considered, we do not recommend to lift schools closure in this region during May or, at most, to target the 25% scenario at the beginning of June but only when authorities can ensure the implementation of a moderate cti strategy.

We end with some final remarks and mentioning some of our future works:

- Since April 28 Chilean government has modified the way to compute and report the daily number of infected [9]. They now report symptomatic and asymptomatic cases due to a change in the detection strategy, consisting (until now) in seeking asymptomatic cases in some confined places, such as jails, nursing homes, etc. This had led to an important increment in the number of daily infected that cannot be predicted by our model. Moreover, this new detection methodology is not compatible with our assumption on the infected stage I, which considers that only symptomatic cases are detected. However, since this change is very new, and there are no enough historical data regarding asymptomatics, we have decide to keep working with our 8-stages model for this report. A new model which includes more stages, such as detected-asymptomatic cases, will be considered in future reports.

- Our model does not consider important consequences in the dynamics and health population due to the related economic crisis triggered by the COVID-19 outbreak. This phenomenon is of independent interest, and will be considered in forthcoming reports.

- Monitoring and analyzing each region as a specific case would provide rich information in order to design and implement measures tailored to each specific context. Certainly, more disaggregated data would allow analysis of smaller geographic areas, with their particularities, providing more detailed information for the application of specific measures. Unfortunately, information at the municipality or district level is not delivered on a daily basis, and information at a more disaggregated level is not reported.

References

[1] Considerations for School Closure. https://www.cdc.gov/coronavirus/2019-ncov/downloads/considerations-for-school-closure.pdf. Accessed: 2020-04-06.

[2] Google COVID-19 Community Mobility Reports. https://www.google.com/covid19/mobility/. Accessed: 2020-04-30.

[3] X. Aguilera, C. Araos, R. Ferreccio, F. Otaiza, G. Valdivia, M. T. Valenzuela, P. Vial, and M. O'Ryan. Consejo Asesor COVID-19 Chile, 03 2020. URL: https://sites.google.com/udd.cl/consejocovid19chile/p%C3%A1gina-principal.

[4] F. Brauer and C. Castillo-Chávez. *Mathematical models in population biology and epidemiology*, volume 40 of *Texts in Applied Mathematics*. Springer-Verlag, New York, 2001. URL: https://doi-org.usm.idm.oclc.org/10.1007/978-1-4757-3516-1, doi:10.1007/978-1-4757-3516-1.

[5] A. Cancino, C. Castillo, T. De Wolff, P. Gajardo, R. Lecaros, C. Muñoz, J. Ortega, and H. Ramírez. Report #4: : Estimation of maximal ICU beds demand for COVID-19 outbreak in some Chilean regions and the effects of different mitigation strategies. Technical report, CMM-AM2V-CEPS, 03 2020. URL: http://covid-19.cmm.uchile.cl/.

[6] A. Cancino, C. Castillo, P. Gajardo, R. Lecaros, C. Muñoz, C. Naranjo, J. Ortega, and H. Ramírez. Report #2: Estimation of maximal ICU beds demand for COVID-19 outbreak in Santiago, Chile. Technical report, CMM-AM2V-CEPS, 03 2020. URL: http://covid-19.cmm.uchile.cl/.

[7] A. Cancino, C. Castillo, P. Gajardo, R. Lecaros, C. Muñoz, J. Ortega, and H. Ramírez. Report #3: Estimation of maximal ICU beds demand for COVID-19 outbreak in Santiago (Chile) and the effects of different mitigation strategies. Technical report, CMM-AM2V-CEPS, 03 2020. URL: http://covid-19.cmm.uchile.cl/.

[8] A. Cancino, P. Gajardo, R. Lecaros, C. Muñoz, J. Ortega, and H. Ramírez. Report #1: Estimation of maximal ICU beds demand for COVID-19 outbreak in Santiago, Chile. Technical report, CMM-AM2V, 03 2020. URL: http://covid-19.cmm.uchile.cl/.

[9] Ministerio de Salud Chile. Cifras Oficiales COVID-19 Chile, 04 2020. URL: https://www.gob.cl/coronavirus/cifrasoficiales/.

[10] O. Diekmann, H. Heesterbeek, and T. Britton. *Mathematical tools for understanding infectious disease dynamics*, volume 7. Princeton University Press, 2012.

[11] España Equipo COVID-19. RENAVE. CNE. CNM (ISCIII). Informe #23: : Situación de covid-19 en españa a 16 de abril de 2020. Technical report, Red Nacional de Vigilancia Epidemiológica, Gobierno de España, 04 2020. URL: https://www.isciii.es/QueHacemos/Servicios/VigilanciaSaludPublicaRENAVE/EnfermedadesTransmisibles/Paginas/InformesCOVID-19.aspx.

[12] The Organisation for Economic Co-operation and Development. Flattening the covid-19 peak:containment and mitigation policies. Technical report, 03 2020. URL: https://read.oecd-ilibrary.org/view/?ref=124_124999-yt5ggxirhc&Title=Flattening.

[13] X. He, E. H. Y. Lau, P. Wu, X. Deng, J. Wang, X. Hao, Y. C. Lau, J. Y. Wong, Y. Guan, X. Tan, X. Mo, Y. Chen, B. Liao, W. Chen, F. Hu, Q. Zhang, M. Zhong, Y. Wu, L. Zhao, F. Zhang, B. J. Cowling, F. Li, and G. M. Leung. Temporal dynamics in viral shedding and transmissibility of covid-19. *Nature Medicine*, 2020. URL: https://doi.org/10.1038/s41591-020-0869-5, `doi:10.1038/s41591-020-0869-5`.

[14] B. Ivorra, M.R. Ferrández, M. Vela-Pérez, and A.M. Ramos. Mathematical modeling of the spread of the coronavirus disease 2019 (COVID- 19) considering its particular characteristics. The case of China. Technical report, MOMAT, 03 2020. URL: https://doi-org.usm.idm.oclc.org/10.1007/s11538-015-0100-x.

[15] K. Prem, A. R. Cook, and M. Jit. Projecting social contact matrices in 152 countries using contact surveys and demographic data. *PLoS computational biology*, 13(9):e1005697, 2017.

[16] J. Riou, A. Hauser, M. J. Counotte, and C. L. Althaus. Adjusted age-specific case fatality ratio during the covid-19 epidemic in hubei, china, january and february 2020. *medRxiv*, 2020. URL: https://www.medrxiv.org/content/10.1101/2020.03.04.20031104v1?versioned=true.

[17] T. W. Russell, J. Hellewell, S. Abbott, H. Gibbs N. Golding, C. I. Jarvis, K. van Zandvoort, CMMID nCov working group, S. Flasche, R. M. Eggo, W. J. Edmunds, and A. J. Kucharski. Using a delay-adjusted case fatality ratio to estimate under-reporting. Technical report, CMMID, 03 2020. Last updated: 2020-04-30. URL: https://cmmid.github.io/topics/covid19/global_cfr_estimates.html.

[18] R. M. Viner, S. J. Russell, H. Croker, J. Packer, J. Ward, C. Stansfield, O. Mytton, C. Bonell, and R. Booy. School closure and management practices during coronavirus outbreaks including covid-19: a rapid systematic review. *The Lancet Child & Adolescent Health*, 2020.